Magnetic ordering and the role of superexchange Ni–O–B–O–Ni upon the formation of magnetic order in ludwigite Ni_2MnBO_5 from first-principal calculations[☆]

Svetlana Sofronova [*], Artem Chernyshev

Kirensky Institute of Physics of the Federal Research Center "Krasnoyarsk Science Center of the Siberian Branch of the Russian Academy of Sciences", 660036, Krasnoyarsk, Russia

ABSTRACT

The energies of various magnetically ordered structures for ludwigite Ni_2MnBO_5 have been calculated in the framework of the first-principles approach using the Wien2K program package, with the parameters of exchange interactions being determined. Two subsystems can be distinguished in the magnetic system, which are associated with the triads 4-2-4 and 3-1-3. The magnetic moments of the ions in both triads are antiferromagnetically oriented. The analysis of the exchange contribution to the energy shows that there occurs an increase of the magnetic cell relative to the crystallographic one due to antiferromagnetic ordering of the magnetic moments along the c axis in three-legged ladders formed by 4-2-4 triads. However, in three-legged ladders formed by 3-1-3 triads, the magnetic moments of the ions are ordered along the c-axis ferromagnetically. The predicted type of magnetic ordering in Ni_2MnBO_5 is similar to magnetic ordering in Fe_3BO_5. Non-collinear ordering of the magnetic moments of the subsystems at different temperatures is also likely to be observed in Ni_2MnBO_5, as is the case in Fe_3BO_5. Superexchange (indirect) interactions (No-O-B-O-Ni) influence the orientation of the magnetic moments of two 3-1-3 (4-2-4) triads within the unit cell. It is these interactions that may be responsible for the formation of long-range magnetic order in Co_3BO_5 and ferrimagnetic-antiferromagnetic spin-reorientation transition in Fe_3BO_5.

1. Introduction

Oxyborates $(Ni,Mn)_3BO_5$ were first obtained in the 1990s [1,2]. The synthesis of the crystal structure of $Ni_5Mn(BO_5)_2$ of the ludwigite type and its study were presented in Ref. [2]. Though, the physical properties of this compound have not been studied yet. According to the electrical neutrality condition, the valence state of manganese ions in $Ni_5Mn(BO_5)_2$ is 4+. However, manganese ions in compounds with the ludwigite structure can have other valence states, e.g. ludwigite Mn_3BO_5, in which manganese ions are in the di- and trivalent state [3]. Recently, a number of $(Ni,Mn)_3BO_5$ compounds with different content of nickel and manganese ions have been obtained at the Institute of Physics SB RAS, with their structural and magnetic properties being studied [4–6]. For example, a magnetization reversal effect is observed in the $Ni_{1.2}Mn_{1.8}BO_5$ compound in low fields, which indicates the existence of at least two magnetic subsystems coupled to each other

antiferromagnetically [5]. In ludwigite Ni_2MnBO_5, manganese ions are in the trivalent state, while in $Ni_{2.14}Mn_{0.86}BO_5$ some of the manganese ions are in the tetravalent state. However, despite the fact that the chemical disorder in $Ni_{2.14}Mn_{0.86}BO_5$ is higher than that in Ni_2MnBO_5, the temperature of magnetic ordering is also higher [7,8].

It has been shown in various studies that in ludwigites there arise a lot of competing interactions due to geometric features of the crystal structure, which leads to the fact that the magnetic system is divided into two subsystems [9–13]. The studies of magnetic ordering by neutron diffraction show that in ludwigites Fe_3BO_5 and Cu_2MnBO_5 there are two magnetic subsystems, similar to three-legged ladders, whose magnetic moments are oriented non-collinearly [9,10,14,15]. In Fe_3BO_5, the magnetic subsystems are ordered at different temperatures while in Cu_2MnBO_5, a single magnetic phase transition is observed. In addition, a structural phase transition is observed in Fe_3BO_5, which is associated with one of the subsystems and leads to the cell doubling
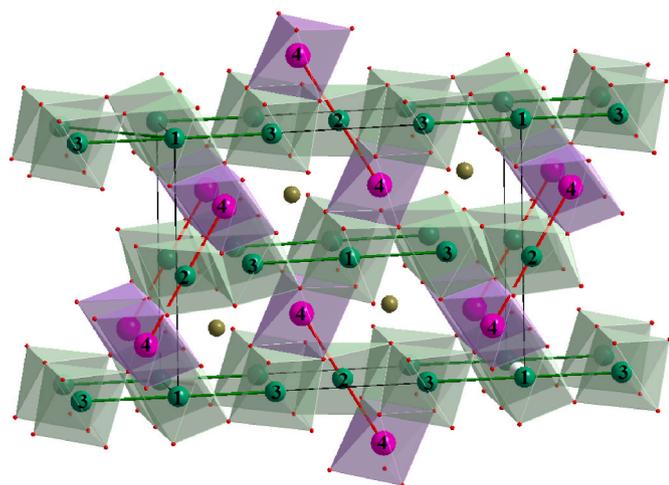
Fig. 1. The ludwigite structure. The transition metal ions in position 2a (1), 2d (2), 4g (3) are denoted by green circles, and positions 4h (4) are shown by magenta circles. The subsystems forming triads 4-2-4 and 3-1-3 are shown by red and green lines. (For interpretation of the references to colour in this figure legend, the reader is referred to the Web version of this article.)
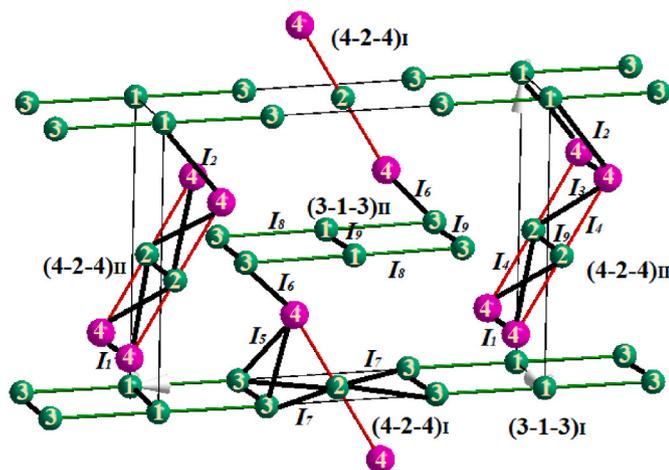
Fig. 2. The crystal structure of ludwigite Ni_2MnBO_5. I_1–I_9 – exchange coupling parameters within the first coordination sphere. The triads of each type are indicated: $(4\text{-}2\text{-}4)_I$, $(4\text{-}2\text{-}4)_{II}$ and $(3\text{-}1\text{-}3)_I$, $(3\text{-}1\text{-}3)_{II}$.

along one of the axes [13,16,17]. In Cu_2MnBO_5, the magnetic cell coincides with the crystallographic one, and no structural phase transition is observed [14].

In our previous work the constants of exchange interactions were determined within the framework of a semi-empirical approach. It was shown that in ludwigite Ni_2MnBO_5 an increase in the magnetic cell was not beneficial [7]. In this study, we have determined the exchange interaction constants by calculating the energies of various magnetically ordered states using the Wien2k software package. We have specified the most favorable type of magnetic ordering in Ni_2MnBO_5 by estimating the exchange contribution to the energy, and also showed that it is necessary to take superexchange (indirect) interactions into account.

2. Theoretical calculations

The crystal structure of ludwigite is shown in Fig. 1. Transition metal ions occupy 4 crystallographic positions: 2a (1 in Fig. 1), 2d (2 in Fig. 1), 4g (3 in Fig. 1) and 4h (4 in Fig. 1). As a rule, position 4 is occupied by trivalent cations, while positions 1–3 – by bivalent ones. The X-ray diffraction method does not allow determining the distribution of nickel

Table 1

The exchange coupling parameters within the first coordination sphere in the ludwigite structure.

Exchange coupling parameters	Position	Me_i-Me_j	Angles of indirect exchange interaction, Me–O–Me
I_1	4–4	Mn–Mn	90°
I_2	4–1	Mn–Ni	90°
I_3	4–2	Mn–Ni	180°
I_4	4–2	Mn–Ni	90°
I_5	3–4	Ni–Mn	90°
I_6	3–4	Ni–Mn	120°
I_7	3–2	Ni–Ni	90°
I_8	3–1	Ni–Ni	120°
I_9	3–3	Ni–Ni	90°
	2–2	Ni–Ni	90°
	1–1	Ni–Ni	90°

and manganese ions across the positions since these ions have a similar electron configuration. However, the ion distribution across the positions can be inferred from the local environment of the transition metal ions. Our experimental research of the local structure of Ni_2MnBO_5 by the XANES method in Refs. [7,8] shows the oxygen octahedron around the ions in position 4 to be highly distorted, i.e. it is elongated along one axis, which is typical for trivalent manganese ions. On the other hand, the oxygen octahedra in positions 2 and 3 are slightly squashed, which is typical for bivalent nickel ions in the octahedral environment. The oxygen octahedron around the ion in position 1 is almost symmetrical; we assume positions 1–3 to be predominantly occupied by nickel ions and position 4 to be occupied by trivalent manganese ions. Thus, in theoretical calculations we will assume that positions 1–3 are occupied by nickel ions, and position 4 is occupied by manganese ions.

As noted earlier, in ludwigites the magnetic system tends to be divided into two subsystems: the first one is formed by ions in positions 4 and 2, and the second one by ions in positions 3 and 1. The ions in the subsystems form triads 4-2-4 and 3-1-3 (shown by red and green lines in Fig. 1), which are repeated along the c axis to form three-legged ladders. Subsystem 3-1-3 is formed by bivalent Ni ions while subsystem 4-2-4 is formed by trivalent Mn ions and bivalent Ni ions. The unit cell contains two triads of each type (Figs. 1 and 2), with these being designated $(4\text{-}2\text{-}4)_I$, $(4\text{-}2\text{-}4)_{II}$ and $(3\text{-}1\text{-}3)_I$, $(3\text{-}1\text{-}3)_{II}$ in Fig. 2.

Within the framework of semi-empirical calculations, the ludwigite structure can be characterized by eleven exchange coupling parameters (Fig. 2, Table 1), three of them (1-1, 2-2, 3-3) characterize the exchange interaction of nickel ions in chains along the c axis, which are formed by ions in positions 1, 2 and 3. Since the distances between the nickel ions in all three chains are the same, we assume that these three parameters are also the same. Thus, within the framework of the first-principles approach, we determine nine parameters of the exchange coupling, with the information being given in Table 1. As can be seen from Figs. 1 and 2, as well as from Table 1, the exchange bonds between the ions in positions 3 and 1 form an angle of about 120°. In the 3-1-3 subsystem, the oxygen octahedra are connected by vertices along the 3-1-3 triad and edges along the c axis. In the 4-2-4 subsystem, the oxygen octahedra are connected by edges both along the 4-2-4 triad and along the c axis, forming 90° exchange bonds. In addition to 90° exchange coupling between the ions in positions 4 and 2 in one cell, 180° exchange coupling between the ions in positions 4 and 2 in adjacent cells is possible.

To determine the exchange coupling parameters, we calculated the energy of various magnetically ordered structures using the Wien2k software package. In the Wien2K software package, use is made of the method of linearized augmented plane waves with local orbitals [18–20]. The exchange-correlation energy is calculated in the LSDA approximation [21] taking into account the density gradient [22], and Hubbard correlation coefficients. In our calculations, we used the potentials $U = 0.52$ Ry and $J = 0$ Ry [23,24]. In estimating the total energy, a set of 400 k-points in the Brillouin zone was employed, and the value $R_{mt}K_{max} = 7.0$. The energy calculation accuracy was 1 μRy. The
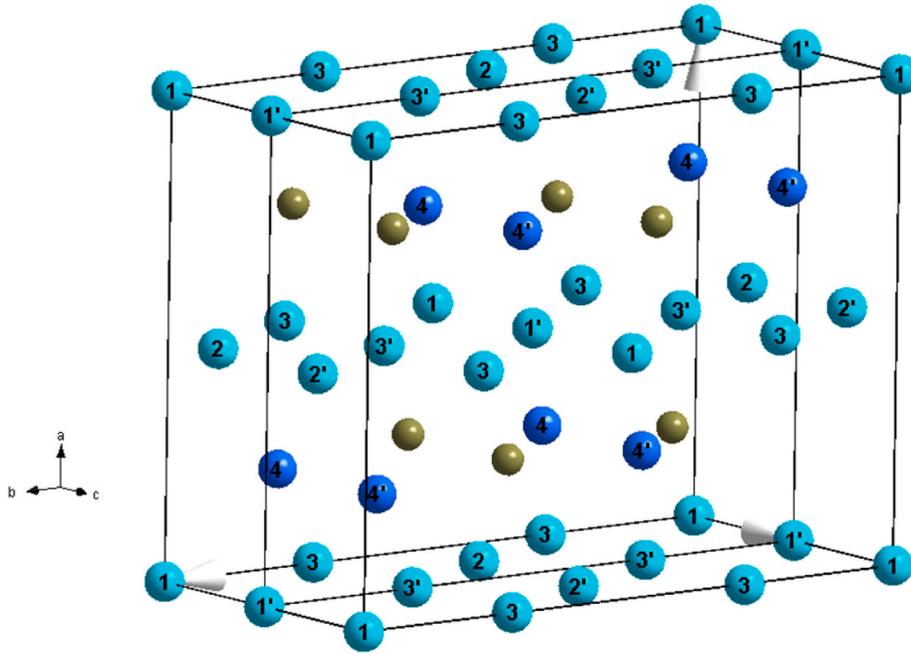
Fig. 3. The crystal cell doubled along the c axis.

Table 2
The calculated energy of different magnetically ordered structures, direction of the magnetic moments on the atoms, and expression of the exchange contribution to the energy.

N°	Direction of the magnetic moments on the atoms[a]				Expression of the exchange contribution to the energy	Calculated energy (Ry)
	1	2	3	4		
Magnetic cell coinciding with the crystallographic one						
1	d u	u u	u u d d	d d u d	$8I_1-4I_2-2I_3-2I_4-4I_5+4I_6-4I_8+12I_9$	−36810,048891
2	u d	u u	u u d d	u d u u	$8I_1+4I_2+2I_3+2I_4-4I_5+4I_6+4I_8+12I_9$	−36810,054295
3	d d	d d	d d d d	d d u u	$8I_1+4I_2+2I_3+2I_4+4I_5+4I_6+8I_7+4I_8+12I_9$	−36810,052532
4	u u	u d	u u u u	u u u d	$8I_1+4I_2+2I_3+2I_4+4I_5+4I_6+4I_8+12I_9$	−36810,052481
5	u d	u u	d d u u	u u u d	$8I_1-4I_2+2I_3+2I_4-4I_5+4I_6-4I_8+12I_9$	−36810,007498
6	u d	u d	u d d u	d u u d	$8I_1-8I_5+8I_6+12I_9$	−36810,050238
7	u u	u u	u u u u	u u u u	$8I_1+8I_2+4I_3+4I_4+8I_5+8I_6+8I_7+4I_8+12I_9$	−36810,054161
Magnetic cell doubled along the c axis						
	1/1′	2/2′	3/3′	4/4′	Expression of the exchange contribution to the energy	Calculated energy (Ry)
8	u u/d d	d u/d d	u u u u/d d d d	d d u u/d d d d	$8I_4+8I_8-12I_9$	−73619,974725
9	u u/d d	u d/d d	u u u u/d d d d	d d u u/d d d d	$8I_8-12I_9$	−73619,960198
10	u u/d d	d d/d d	u u u u/d d d d	u u u u/u u u u	$8I_1-8I_3-8I_4+8I_8-8I_9$	−73619,957818
11	u u/d d	u u/d d	d d d d/u u u u	d d d d/u u u u	$-8I_1+8I_3-8I_4-8I_8-16I_9$	−73619,996122
12	u d/u d	u u/u u	d d u u/d d u u	d d d d/d d d d	$8I_1-8I_3-8I_4-8I_8+16I_9$	−73619,962918
13	u d/u d	u d/u d	d d u u/d d u u	d d d d/u u u u	$-8I_1-16I_7-8I_8+16I_9$	−73619,995846
14	u u/d d	u d/d d	d d u d/d d d d	d u d u/d d d d	$4I_4+4I_5+4I_6+4I_7+2I_8$	−73619,980563
15	u u/d d	d d/d d	d d d u/d u u d	d d u d/d u u u	$4I_5-4I_6+4I_7-2I_8-4I_9$	−73619,977345
16	d d/u d	u u/u u	d d u d/u d u u	d u u d/u d d u	$-8I_1+4I_9$	−73619,975695

(0 0 0) (½ ½ 0), 2: (0 ½ ½) (½ 0 ½), 3: (-x -y z) (x y z) (½-x ½+y -z) (x-½ ½-y -z),
(-x -y z) (x-½ ½-y -z) (½-x ½+y -z) (x y z).
[a] Coordinates of the ions in the magnetic cell coinciding with the crystallographic one.

following radii of atomic spheres were used in the calculations: 2.02 at. units for nickel ions, 2.02 at. units for cobalt ions, and 1.30 at. units for boron and oxygen ions. The modified Blöchl tetrahedral method was applied to calculate the total density of the states [25].

The lattice parameters and atomic coordinates do not change in calculating the energies of various magnetically ordered structures, while the magnetic configuration changes. In this approach, the energy can be divided into the exchange contribution and a constant that includes all other interactions.

$$E_m = -\frac{1}{2}\sum_{ij} J_{ij}\langle s_i \cdot s_j \rangle + e_0,$$

Table 1 shows nine exchange coupling parameters to be calculated

and the number of positions with coupling; we consider all other parameters of exchange coupling to be equal to zero.

It should be noted that to calculate the exchange coupling parameters I_1 and I_9 it is necessary to calculate the energies for magnetic cells doubled along the c axis (Fig. 3), since within the framework of a magnetic cell coinciding with a crystallographic one, their contribution cannot be distinguished. For ease of perception, we keep the numbering of the doubling positions: 2a (1 and 1′), 2d (2 and 2′), 4g (3 and 3′) and 4f (4 and 4′) in Fig. 3.

Table 2 shows the magnetically ordered structures, direction of the magnetic moments on the atoms, expression of the exchange contribution to the energy through the exchange coupling parameters and calculated energy values. The calculated values of the exchange

Table 3

The calculated exchange coupling parameters (Ry).

I_1	I_2	I_3	I_4	I_5	I_6	I_7	I_8	I_9
$-1,2*10^{-4}$	$-8,5*10^{-4}$	$2,1*10^{-3}$	$1,8*10^{-3}$	$5,0*10^{-4}$	$-5,1*10^{-4}$	$6,2*10^{-6}$	$-2,1*10^{-3}$	$5,8*10^{-5}$

Table 4

The exchange contribution to the energy of various magnetically ordered structures.

N⁰	Direction of the magnetic moments on the atoms				Exchange contribution to the energy (Ry)
	1/1′	2/2′	3/3′	4/4′	
1	u u/ u u	u u/ u	u u u u/ u u u u	u u u u/ u u u u	−0,000570
2	u u/u u	u u/ u	u u u u/ u u u u	d d d d/ d d d d	0,033789
3	d d/ d d	u u/ u	u u u u/ u u u u	d d d d/ d d d d	0,027839
4	u d/ u d	u d/ u	u d u d/ u d u d	d u d u/ d u d u	−0,000180
5	d d/ d d	d u/ u	u u u u/ u u u u	u u d d/ u u d d	−0,016074
6	u u/ d d	u d/ d u	d d d d/ u u u u	d d u u/u u d d	−0,018648
7	u d/ d	u d/ d	d d u u/ d d u u	d d d d/ u u u u	−0,018373
8	u u/ u u	u u/ d d	d d d d/ d d d d	d d d d/ u u u u	−0,020045
9	u d/ d	u d/ d u	d d u u/ d d u u	d d u u/ u u d d	−0,020045
10	u u/ u u	u d/ d u	d d d d/ d d d d	d d u u/ u u d d	−0,020045
11	u d/ d	u u/ d d	d d u u/ d d u u	d d d d/ u u u u	−0,020045

coupling parameters are given in Table 3. Using the obtained exchange coupling parameters, we can calculate the exchange contribution to the energy of any magnetically ordered structure. We considered structures corresponding to eigenvectors for magnetic representations, according to the group-theoretic analysis [15]. The calculated exchange contribution is given in Table 4. In contrast to our previous calculations within the framework of the semi-empirical approach [7], doubling of the magnetic cell is energetically more favorable. For structures 1–4 the magnetic cell coincides with the crystallographic one, for the other ones the magnetic cell is doubled along the c axis. As can be seen from Table 4, four magnetically ordered structures (N⁰ 8–11) have the same contribution to the exchange energy, with this exchange contribution having the maximum value.

Fig. 4 shows these four types of magnetic ordering (N⁰ 8–11). We depicted the magnetic structure of the crystal in Fig. 4 in the form of triads; as is noted earlier, the unit cell contains two triads of each type (3-1-3 and 4-2-4). Since the magnetic cell is doubled along the c-axis, each triad forms a ladder along the c-axis. As can be seen from Fig. 4, in all the most favorable types of magnetic ordering in the 3-1-3 subsystem, the magnetic moments along the c axis are ordered ferromagnetically while in the triad they are ordered antiferromagnetically, but in the 4-2-4 subsystem the magnetic moments are ordered antiferromagnetically both in the triad and along the c axis.

The exchange couplings between the subsystems are antiferromagnetic and form triangular groups, which results in these couplings being strongly frustrated. According to group theoretical analysis, the magnetic moments of triads of the same type can be ordered in a parallel or antiparallel manner [15]. Since the exchange couplings between the triads are frustrated, the energy of the exchange contribution is the same, regardless of how the magnetic moments of triads of the same type are oriented, whether in a parallel or antiparallel manner.

Our approach takes into account only the exchange coupling within the first coordination sphere, without considering, for example, such indirect exchange interactions as Ni–O–B–O–Ni, which can also contribute to the exchange energy. To verify whether other types of
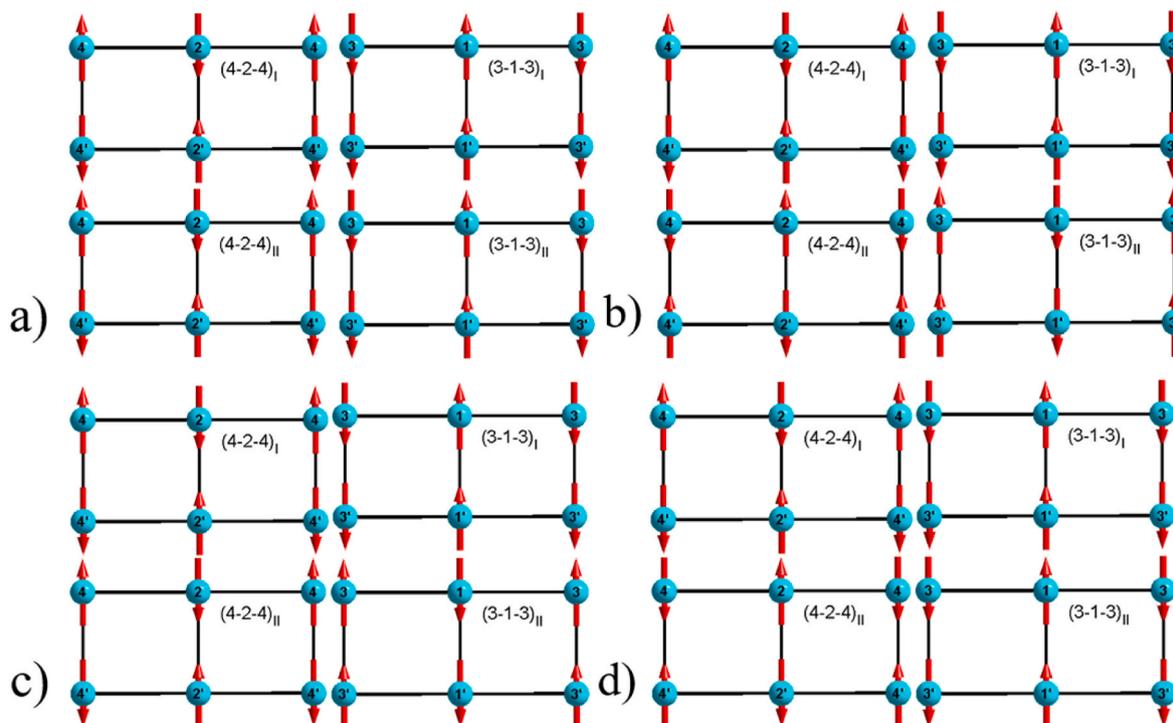
Fig. 4. Magnetic ordering with the lowest exchange contribution to the energy.

Table 5
The calculated energy values for the magnetic structures with the lowest exchange contribution to the energy.

	Orientation of the magnetic moments of (3-1-3)$_I$ and (3-1-3)$_{II}$	Orientation of the magnetic moments of (4-2-4)$_I$ and (4-2-4)$_{II}$	Calculated energy
a	FM	FM	−73619,997519
b	AFM	AFM	−73619,997848
c	AFM	FM	−73619,995712
d	**FM**	**AFM**	**−73619,999523**

exchange interactions have any contribution, we carried out accurate calculations of the energies of the four most favorable types of magnetically ordered structures. The calculation results are given in Table 5. As can be seen from the table, the exact calculation gives different energy values for all the four structures, but the change in the energy values is observed only in the third fraction digit. Thus, we can conclude that in ludwigites, the exchange interactions in the second coordination sphere also contribute to the energy, although by an order of magnitude lower than the contribution from the exchange interactions in the first coordination sphere. In Ni_2MnBO_5, these weak exchange bonds yield the most favorable ferrimagnetic structure when in the crystal cell both 3-1-3 triads are oriented in the same way, and the 4-2-4 triads are antiferromagnetic (see Fig. 5).

It is interesting to note that in Co_3BO_5, the trivalent cobalt ions occupying position 4 are in the low-spin state and their magnetic moment is equal to zero [26]. Examining the structure of ludwigite, one can see that the ions in position 4 are located between the planes formed by the ions in positions 1, 2 and 3 (Fig. 6). In Co_3BO_5, the exchange interaction between the planes is possible through indirect superexchange interactions Co–O–B–O–Co, and two exchange paths are possible: Co$_3$–O–B–O–Co$_1$ and Co$_3$–O–B–O–Co$_3$ (Fig. 6). The magnetic transition to the ferrimagnetic state in Co_3BO_5 is observed at 42 K, which is much lower than in ludwigite Fe_3BO_5, where magnetic ordering occurs in two stages: at 112 K and 74 K. In ludwigite Fe_3BO_5, the transition to the antiferromagnetic state occurs at 112 K and the subsystem is ordered as 4-2-4, while at 74 K one observes the transition into the

ferrimagnetic state, and the 3-1-3 subsystem is ordered. According to the neutron diffraction data in Fe_3BO_5, both 3-1-3 triads in the unit cell are parallel oriented. However, in the field dependences of magnetization in the region of 40 K, hysteresis loops disappear and at low temperatures the behavior of magnetization becomes antiferromagnetic [27]. It is possible that in the region of 40 K there occurs a spin-reorientation transition and two 3-1-3 triads in the cell are antiparallel oriented. It is interesting to note that the spin reorientation transition and ordering in Co_3BO_5 occurs at similar temperatures, which may indicate that in this temperature range the Fe–O–B–O–Fe superexchange interactions are sufficient to affect the magnetic order in Fe_3BO_5. The superexchange interactions also couple subsystem 4 (Me$_4$–O–B–O–Me$_4$), affecting the orientation of the magnetic moments of the 4-2-4 triads.

It is not possible to calculate the energy of a non-collinear magnetic structure using the Wien2k software package. However, the similarity
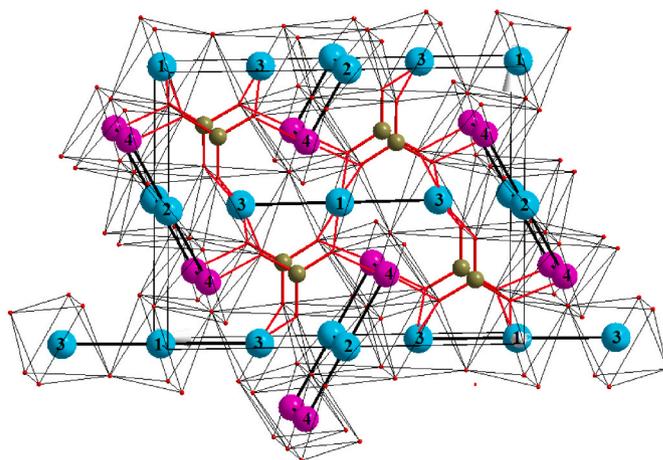
Fig. 6. The ludwigite structure. The superexchange interactions Me–O–B–O–Me are shown by red line. (For interpretation of the references to colour in this figure legend, the reader is referred to the Web version of this article.)
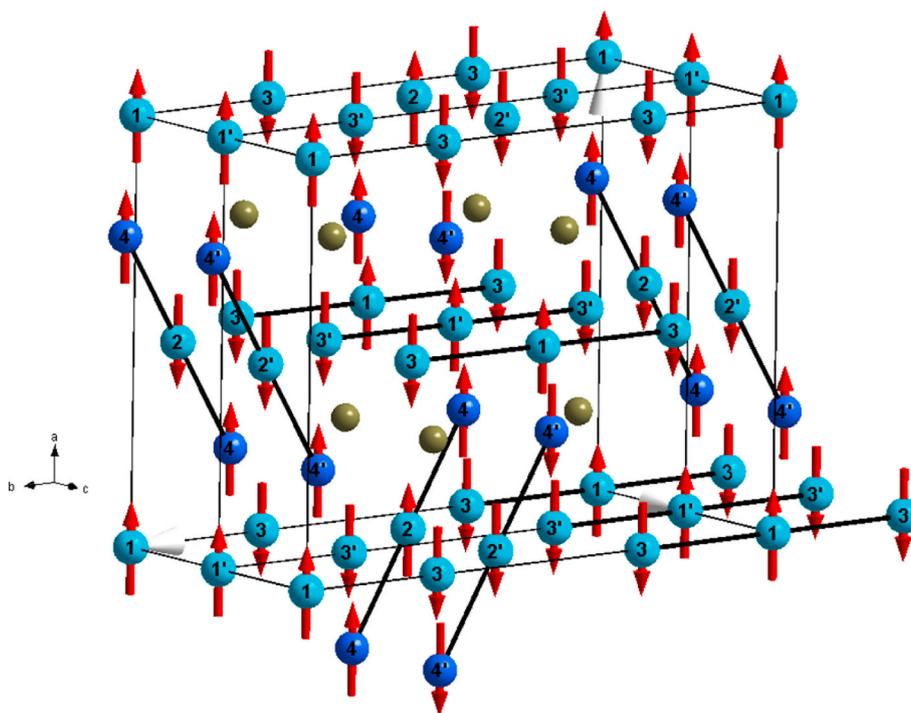
Fig. 5. The most favorable ferrimagnetic structure in Ni_2MnBO_5.

between the magnetic structure obtained for Ni_2MnBO_5 and the magnetic structure of Fe_3BO_5 allows one to assume that in Ni_2MnBO_5 there are also two magnetic subsystems that are ordered non-collinearly at different temperatures. Two features are observed in the experimental dependences of the magnetization of Ni_2MnBO_5 [7]. In our latest studies, where we investigated the $(Ni,Mn,Cu)_3BO_5$ solid solutions with small copper content, features in the temperature dependences of the ac-susceptibility measured upon the magnetic field applied along and perpendicular to the c axis, are observed at different temperatures [28]. Apparently, the ludwigites are characterized by the presence of two magnetic subsystems, which are ordered non-collinearly due to the geometric features of the structure.

3. Conclusion

In this study we estimated the parameters of exchange coupling of the first coordination sphere by calculating the energies of various magnetically ordered structures of Ni_2MnBO_5. The calculation of the exchange contribution to the energy using the obtained exchange coupling parameters shows that the magnetic cell is doubled along the c axis due to antiferromagnetic ordering in the 4-2-4 subsystem. The magnetic moments in the 4-2-4 subsystem are oriented antiferromagnetically both in the triad and along the c axis, while in the 3-1-3 subsystem the magnetic moments in the triad are oriented both antiferromagnetically and ferromagnetically along the c axis. Due to the fact that the exchange interactions between the subsystems form triangular groups, they are greatly frustrated. If, when calculating the exchange contribution, we take into account only the exchange interactions of the first coordination sphere, then due to the frustration of the exchange interactions between the subsystems, the exchange contribution to the energy will not depend on the mutual orientation of the magnetic moments of triads of the same type. However, the accurate calculation of the energy shows that the mutual orientation of the magnetic moments of triads of the same type affects the energy. The triads of the same type are coupled by superexchange interactions through oxygen and boron ions, and although the contribution to the energy from superexchange interactions is an order of magnitude lower, it can be significant at low temperatures. It is likely that superexchange interactions play a key role in the establishment of long-range magnetic order in Co_3BO_5 and in the occurrence of a spin-reorientation transition in Fe_3BO_5.

CRediT authorship contribution statement

Svetlana Sofronova: Writing – review & editing, Writing – original draft, Visualization, Validation, Supervision, Investigation, Formal analysis, Data curation, Conceptualization. **Artem Chernyshev:** Visualization, Investigation, Formal analysis, Data curation.

Declaration of competing interest

The authors declare that they have no known competing financial interests or personal relationships that could have appeared to influence the work reported in this paper.

Data availability

Data will be made available on request.

References

[1] K. Bluhm, H. Müller-Buschbaum, About the stabilization of the oxidation state M^{IV} in the $Ni_5MB_2O_{10}$-type ($M=V^{4+}$, Mn^{4+}), Z. Anorg. Allg. Chem. 579 (1989) 111–115.

[2] K. Bluhm, H. Müller-Buschbaum, Oxometallate mit inselförmigen bor-einlagerungen $Ni_5MB_2O_{10}$, J. Less Common Met. 147 (1989) 133–139.

[3] A. Utzolino, K. Bluhm, Neue einsichten zur stabilisierung des hulsit-strukturtyps am beispiel von Mn(ii)$_2$Mn(iii)(BO$_3$)O$_2$ und Mn(ii)Sr Mn(iii) (BO$_3$)O2, Z. Naturforsch., B: Chem. Sci. 51 (1996) 1433–1438.

[4] L. Bezmaternykh, E. Moshkina, E. Eremin, M. Molokeev, N. Volkov, Y. Seryotkin, Spin-lattice coupling and peculiarities of magnetic behavior of ferrimagnetic ludwigites $Mn_{0.52}M_{1.52}Mn^{3+}BO_5$(M=Cu, Ni), Solid State Phenom. 233–234 (2015) 133–136.

[5] L.N. Bezmaternykh, E.M. Kolesnikova, E.V. Eremin, S.N. Sofronova, N.V. Volkov, M.S. Molokeev, Magnetization pole reversal of ferrimagnetic ludwigites $Mn_{3-x}Ni_xBO_5$, J. Magn. Magn Mater. 364 (2014) 55–59.

[6] E. Moshkina, A. Bovina, M. Molokeev, A. Krylov, A. Shabanov, A. Chernyshov, S. Sofronova, Study of flux crystal growth peculiarities, structure and Raman spectra of double $(Mn,Ni)_3BO_5$ and triple $(Mn,Ni,Cu)_3BO_5$ oxyborates with ludwigite structure, CrystEngComm 23 (2021) 5624–5635.

[7] E. Moshkina, S. Sofronova, A. Veligzhanin, M. Molokeev, I. Nazarenko, E. Eremin, L. Bezmaternykh, Magnetism and structure of Ni_2MnBO_5 ludwigite, J. Magn. Magn Mater. 402 (2016) 69–75.

[8] S. Sofronova, E. Moshkina, I. Nazarenko, A. Veligzhanin, M. Molokeev, E. Eremin, L. Bezmaternykh, Chemical disorder reinforces magnetic order in ludwigite (Ni, Mn)$_3$BO$_5$ with Mn^{4+} inclusion, J. Magn. Magn Mater. 465 (2018) 201–210.

[9] J. P. Attfield, J. F. Clarke and D. A. Perkins, Magnetic and crystal structures of iron borates// Phys. B Condens. Matter - vols. 180–181 - pp. 581-584.

[10] P. Bordet, E. Suard, Magnetic structure and charge ordering in Fe_3BO_5: a single-crystal x-ray and neutron powder diffraction study, Phys. Rev. B 79 (2009) 144408.

[11] M. Matos, J. Terra, D.E. Ellis, A.S. Pimentel, First principles calculation of magnetic order in a low-temperature phase of the iron ludwigite, J. Magn. Magn Mater. 374 (2015) 148–152.

[12] M.-H. Whangbo, H.-J. Koo, J. Dumas, M.A. Continentino, Theoretical investigation of the spin exchange interactions and magnetic properties of the homometallic ludwigite $Fe_3O_2BO_3$, Inorg. Chem. 41 (2002) 2193–2201.

[13] E. Vallejo, M. Avignon, Spin ordering in three-leg ladders in Ludwigite systems, J. Magn. Magn Mater. 310 (2007) 1130–1132.

[14] E. Moshkina, C. Ritter, E. Eremin, S. Sofronova, A. Kartashev, A. Dubrovskiy, L. Bezmaternykh, Magnetic structure of Cu2MnBO5 ludwigite: thermodynamic, magnetic properties and neutron diffraction study, J. Phys. Condens. Matter 29 (2017) 245801.

[15] S. Sofronova, E. Moshkina, I. Nazarenko, Y. Seryotkin, S.A. Nepijko, V. Ksenofontov, K. Medjanik, A. Veligzhanin, L. Bezmaternykh, Crystal growth, structure, magnetic properties and theoretical exchange interaction calculations of Cu_2MnBO_5, J. Magn. Magn Mater. 420 (2016) 309–316.

[16] R.B. Guimarães, M. Mir, J.C. Fernandes, M.A. Continentino, H.A. Borges, G. Cernicchiaro, M.B. Fontes, E. Baggio-Saitovitch, Cation-mediated interaction and weak ferromagnetism in $Fe_3O_2BO_3$, Phys. Rev. B 60 (1999) 6617.

[17] D.C. Freitas, M.A. Continentino, R.B. Guimarães, J.C. Fernandes, J. Ellena, L. Ghivelder, Structure and magnetism of homometallic ludwigites: $Co_3O_2BO_3$ versus $Fe_3O_2BO_3$, Phys. Rev. B 77 (2008) 184422.

[18] E. Sjöstedta, L. Nordströma, D. Singhb, An alternative way of linearizing the augmented plane-wave method, Solid State Commun. 114 (2000) 15–20.

[19] P. Blaha, K. Schwarz, G. Madsen, D. Kvasnicka, J. Luitz, An Augmented Plane Wave + Local Orbitals Program for Calculating Crystal Properties, Vienna University of Technology Inst. of Physical and Theoretical Chemistry, Vienna, 2015.

[20] P. Blaha, K. Schwarz, F. Tran, R. Laskowski, G. Madsen, L. Marks, WIEN2k: an APW +lo program for calculating the properties of solids, J. Chem. Phys. 152 (2020) 074101.

[21] J. Perdew, Y. Wang, Accurate and simple analytic representation of the electron-gas correlation energy, Phys. Rev. B 45 (1992) 13244.

[22] J.P. Perdew, K. Burke, M. Ernzerhof, Generalized gradient approximation made simple, Phys. Rev. Lett. 77 (18) (1996) 3865.

[23] V.I. Anisimov, J. Zaanen, O.K. Andersen, Band theory and mott insulators: hubbard U instead of stoner I, Phys. Rev. B 44 (1991) 943.

[24] V.I. Anisimov, I.V. Solovyev, M.A. Korotin, M.T. Czyżyk, G.A. Sawatzky, Density-functional theory and NiO photoemission spectra, Phys. Rev. B 48 (1993) 16929.

[25] P.E. Blöchl, O. Jepsen, O.K. Andersen, Improved tetrahedron method for Brillouin-zone integrations, Phys. Rev. B 49 (1994) 16223.

[26] D.C. Freitas, C.P.C. Medrano, D.R. Sanchez, R.M. Nuñez, J.A. Rodríguez-Velamazán, M.A. Continentino, Magnetism and charge order in the ladder compound $Co_3O_2BO_3$, Phys. Rev. B 94 (2016) 174409.

[27] J. Bartolomé, A. Arauzo, N.V. Kazak, N.B. Ivanova, S.G. Ovchinnikov, Y. V. Knyazev, I.S. Lyubutin, Uniaxial magnetic anisotropy in $Co_{2.25}Fe_{0.75}O_2BO_3$ compared to $Co_3O_2BO_3$ and $Fe_3O_2BO_3$ ludwigites, Phys. Rev. B 83 (2011) 144426.

[28] S. Sofronova, A. Veligzhanin, E. Eremin, A.V. Chernyshev, A. Kartashev, D. Velikanov, Possible noncollinear magnetism and different valence state of manganese ions in quasi-low-dimensional ludwigites of $(Ni,Cu,Mn)_3BO_5$, Phys. Status Solidi B 260 (2023) 2200457.